Bridging Stress Modeling of Composite Materials Reinforced by Fibers Using Discrete Element Method

Chong Wang, Kellem M. Soares, Luis E. Kosteski

Abstract—The problem of toughening in brittle materials reinforced by fibers is complex, involving all of the mechanical properties of fibers, matrix and the fiber/matrix interface, as well as the geometry of the fiber. Development of new numerical methods appropriate to toughening simulation and analysis is necessary. In this work, we have performed simulations and analysis of toughening in brittle matrix reinforced by randomly distributed fibers by means of the discrete elements method. At first, we put forward a mechanical model of toughening contributed by random fibers. Then with a numerical program, we investigated the stress, damage and bridging force in the composite material when a crack appeared in the brittle matrix. From the results obtained, we conclude that: (i) fibers of high strength and low elasticity modulus are beneficial to toughening; (ii) fibers of relatively high elastic modulus compared to the matrix may result in substantial matrix damage due to spalling effect; (iii) employment of high-strength synthetic fibers is a good option for toughening. We expect that the combination of the discrete element method (DEM) with the finite element method (FEM) can increase the versatility and efficiency of the software developed. The present work can guide the design of ceramic composites of high performance through the optimization of the parameters.

Keywords—Bridging stress, discrete element method, fiber reinforced composites, toughening.

I. INTRODUCTION

IT is well known that addition of ductile fibers into brittle matrix can significantly improve the brittleness of the matrix. However, toughening analysis is very complicated because it involves fiber/matrix interface debonding, fiber pullout, spalling and snubbing effects, besides the mechanical properties of matrix, fiber and fiber/matrix interface as well as fiber geometry. When a crack appears, fibers across the cracked surfaces undertake high load. This load may lead to fibers breakage or extensive spalling in the matrix, then, the fibers lose their contribution to toughening and become ineffective. Therefore, we must account effective fibers in toughening evaluation. Although some computational models and numerical methods for toughening have been suggested [1]-[7], good results comparing with experiments still are scare. This work makes effort to computational modeling of bridging stress contributed by fibers to toughening in brittle matrix at an early stage of crack formation, using the truss-like

C. Wang is with the Federal University of Pampa, Alegrete, RS 97546-550 Brazil (Phone: +55-55-3421-8400 ext. 3032; fax: +55-55-3421-8401; e-mail: wangchong@unipampa.edu.br).

K. M. Soares is with the Integrated Regional University of Alto Uruguai and Missions, Santo Angelo, RS, 98802-470 Brazil (e-mail: kellempv@hotmail.com).

L. E. Kosteski is with the Federal University of Pampa, Alegrete, RS 97546-550 Brazil (e-mail: luiskosteski@gmail.com).

discrete element method (DEM), which is simple in formulation and suitable for brittle materials. In Section II, the truss-like discrete element method and respective constitutive equation of material are introduced. Section III gives toughening model of composite reinforced by randomly distributed fibers. In the followed section, some cases are modeled and the results are compared in terms of damage and bridging stress with variation in fiber material (steel or synthetic), interface strength, and inclined angle of fiber relative to fractured surfaces.
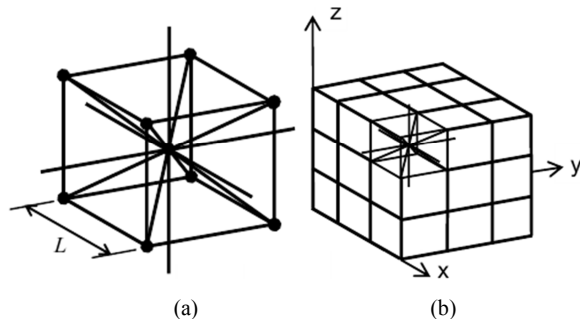

Fig. 1 (a) Core cubic module; (b) Prism composed of several cubic modules

II. THE TRUSS-LIKE DISCRETE ELEMENT METHOD

This approach was proposed by [8] to determine dynamic failure response of concrete plates and shells subjected to impact loads. The truss-like DEM primarily consists of continuous spatial discretization with regular reticulate modules, where the stiffness of a bar is defined in such a way as to be equivalent to the continuum. The cubic mass is discretized and shared by the module nodes. Fig. 1 shows a typical module with nine nodes (eight nodes at the vertices and one at the center). Each node has three freedom degrees representing the spatial components of displacement field u. Longitudinal and diagonal elements with length L_c and $\sqrt{3}L_c/2$ respectively join the masses. A restriction is imposed on the Poisson ratio: $v = 0.25$ for perfect equivalence between the cubic arrangement and the elastic orthotropic solid. For other v values, there are slight differences in the shear terms, but we can ignore it especially when our interest is on the nonlinear response of the model. When the materials have linear elastic behavior, we can express the motion equations of a system with N freedom degrees resulted from the spatial discretization as:

$$\mathbf{M} \cdot \mathbf{u} + \mathbf{K} \cdot \ddot{\mathbf{u}} = \mathbf{q}(t) \tag{1}$$

where **M** denotes the diagonal mass matrix, **u** and **ü** represent displacement and generalized acceleration vectors respectively. On the other hand, the vector **q**(t) contains the applied external forces. The equation system (1) can be numerically integrated in time domain using a classic scheme of explicit integration (Method of Central Finite Differences).

It is important to mention that, for the present applications, using an implicit integration would be more adequate. Since our focus will be on the modeling of toughening in brittle matrix achieved by fibers, in this field, the presented method shows its competence when compared with more classic methods (FEM and BEM).

In the context of DEM there is a way to simulate the fracture and fragmentation of the model. And the constitutive law of the bar has a bilinear shape as presented in Fig. 2 where G_f is associated with the toughness of the material and ε_p is the critical deformation. This allows simulating unstable crack propagation in a natural way. The proposed law permits to accomplish balancing energy during the simulation.
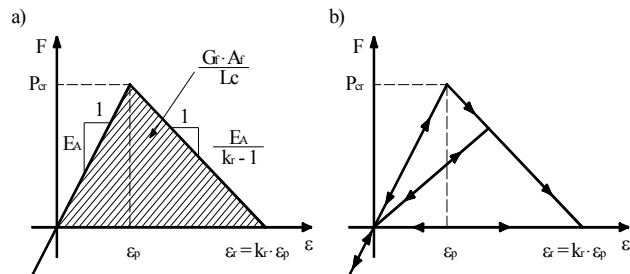

Fig. 2 Constitutive relationship of bar material. a) Adopted constitutive diagram with their control parameters; b) Loading-unloading scheme.

Riera, Iturrioz and Kosteski applied DEM to model the failure of shells subjected to impulsive loads [9]-[11], fracture of elastic foundations on soft sand beds [12], dynamic fracture [13], generation and spread of earthquakes [14], [15], scale effect in concrete [16] and in rock dowels [17], [18]. DEM also was employed to compute static and dynamic mechanics parameters such as stress intensity factors [19]-[20], simulate crack propagation [21]-[23] and predict hardness of stiff materials [24].

III. TOUGHENING MODEL OF COMPOSITE REINFORCED BY RANDOMLY DISTRIBUTED FIBERS

Fig. 3 illustrates the layout of a fiber relative to crack surfaces. The fiber is inclined to the crack surfaces at an angle θ relative to the surface normal. The embedded length of the short part of the fiber is denoted as L_e while the full length as L_f and the fiber diameter as d_f. In terms of geometry we have

$$L_e = L_f/2 - z/cos\theta - L_o. \qquad (2)$$

where z is the distance from the fiber center to the crack surface and the inclined angle θ is limited to:
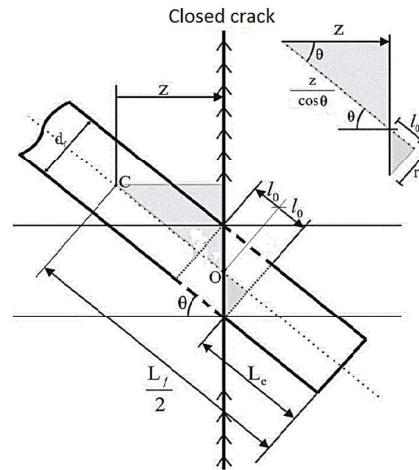
$$\theta \leq arctan(L_f/d_f). \qquad (3)$$

Fig. 3 Configuration of an inclined fiber relative to crack

There are a number of fibers that cross the crack surfaces randomly. Each fiber contributes itself to bridge the two opening surfaces of the crack and intends to keep them from separating. The medium effect of fibers contribution is bridging stress. Just due to this bridging stress, the toughening is achieved. The bridging stress can be determined by the following equation, modifying the one proposed by [3]:

$$\sigma_c(w) = \frac{V_f}{A_f}\int_0^{\theta_f} d\theta \int_0^{z_f} N(w,\theta,z)P(\theta)p(z)dz. \qquad (4)$$

where V_f - volume fraction of fibers; A_f - section area of fiber; $\theta_f = \arctan(L_f/d_f)$, $z_f = (L_f\cos\theta - d_f\sin\theta)/2$, $N(w,\theta,z)$ - the fiber axial force; w - the opening of the surfaces; $P(\theta)$ and $p(z)$ - the distribution functions of fiber inclined angles and fiber center locations respectively, given by

$$P(\theta) = sin\theta \text{ for } 0 \leq \theta \leq \theta_f. \qquad (5)$$

and

$$p(z) = 2/L_f \text{ for } 0 \leq z \leq z_f. \qquad (6)$$

After obtaining the bridging stress, the increment of fracture energy G_c [J/m^2] i.e. toughening can be calculated as the area under the curve of $\sigma_c - w$, using the following integral:

$$G_c = \int_0^{w^*} \sigma_c(w)dw. \qquad (7)$$

where w^* should be the ultimate crack open for which all fiber axial forces become zero, that is, all the fibers are pulled apart or out the matrix.

From (4) we see that to determine the bridging stress, the key is to find the relationship among the axial force of the inclined fiber $N(w,\theta,z)$, the crack open w and the embedded length L_e or the distance from the fiber center to the surface z. This is the major difficulty in toughening simulation, because

one or more of events such as interface debonding, matrix spalling, snubbing effect, fiber pullout or breakage may come about.

Implementing a DEM program in Fortran incorporated with Matlab® and employing post-process of the software ANSYS®, we realized the simulation and got the results.

The program can analyze dynamic problem. Prescription in displacement is imposed by application of velocity and elapsed time, i.e.

$$ds = v.\Delta t. \quad (8)$$

where v is velocity vector (assumed a constant) and Δt the elapsed time.
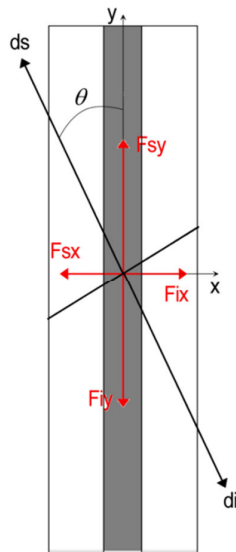
Fig. 4 Coordinate system of reaction force and displacements

The resultant of reaction on the boundary of the left (or right) half matrix (Fig. 3) in the normal direction is equal to bridging force. According to Fig. 4, displacement components can be determined by:

$$ds_y = |ds|cos\theta, ds_x = -|ds|sin\theta,$$

$$di_y = -|di|cos\theta, di_x = |ds|sin\theta. \quad (9)$$

where $|ds| = |di| = w/2$ is a half of crack open.

IV. PARAMETERS AND CASES MODELED

In our simulation, the matrix is cement and fibers are steel or synthetic. In all of cases, the fiber of $10 \times L_c$ in width is centered in a plate with $200 \times L_c$ in length, $54 \times L_c$ in height and $1 \times L_c$ in thickness (Fig. 5). The fiber/matrix interface is of $1 \times L_c$ in width. L_c, the dimension of a cell represented in DEM, is 10 μm. The mechanical properties of the matrix are E=30 GPa, v=0.25, σ_f=3.7 MPa, G_c=24 J/m² and ρ=2500 kg/m³. The other parameters are listed in Table I.
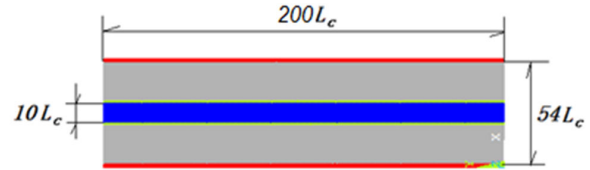
Fig. 5 Dimension of a plate with a centered fiber. Gray represents matrix, blue for fiber, green the interface and red lateral boundary

The studied cases 2, 4, and 5 are of steel fiber while the cases 3 and 6 synthetic fiber. For the cases 2 and 4, the differences are in fiber strength and interface fracture toughness (see the red number in Table I). By comparison, the fiber in the case 5 is stronger than in the case 2 (see the green in Table I). The cases 3 and 6 possess fibers with different strengths (see the brown in Table I).

TABLE I
MATERIAL PARAMETERS USED IN THE INVESTIGATED CASES

Material	Parameter	Case 2	Case 4	Case 5	Case 3	Case 6
Fiber	E (MPa)	200	200	200	60	60
	v	0.3	0.3	0.3	0.35	0.35
	σ_f (MPa)	797	797	1200	2254	1200
	G_c (J/m²)	18000	18000	18000	564	564
	ρ (Kg/m³)	7800	7800	7800	1250	1250
	R (1/$\sqrt{m}$)	12,67	12,67	19,08	363	193,24
Interface	E (MPa)	40	40	40	40	40
	v	0.2	0.2	0.2	0.2	0.2
	σ_f (MPa)	5	2.76	5	5	5
	G_c (J/m²)	16	5	16	16	16
	ρ (Kg/m³)	2800	2800	2800	2800	2800
	R (1/$\sqrt{m}$)	6.053	6.053	6.053	6.053	6.053

V. RESULTS AND ANALYSIS

A. Stress Distribution

Stress distribution is obtained through the post-process of the software ANSYS®. Fig. 6 shows distribution of the Von Mises stress for the case of steel fiber, where u is the applied displacement for which the distribution was plotted while u_q is the one for which no element is broken yet. The value of u_q allows us to know the bar broken comes about early or lately.

Comparing the figures, we can infer that the larger inclination of steel fiber, the earlier the element is broken. This occurs due to existence of high compression between the fiber and the matrix when the fiber is inclined. It can be seen that with no inclination, u_q are 0.05μm, 0.06μm and 0.08μm (see the first column in Fig. 6) respectively for the case 2, 4 and 5; with the 30° inclined angle; these values decrease to 0.02μm, 0.02μm and 0.01μm. When the fiber is inclined at 60°, u_q is only 0.01μm for all of the cases 2, 4 and 5.

From Fig. 6, we conclude that the fiber with high strength (case 5) can undertake larger displacement since high strength permits larger critical deformation if the elasticity module is kept as a constant.
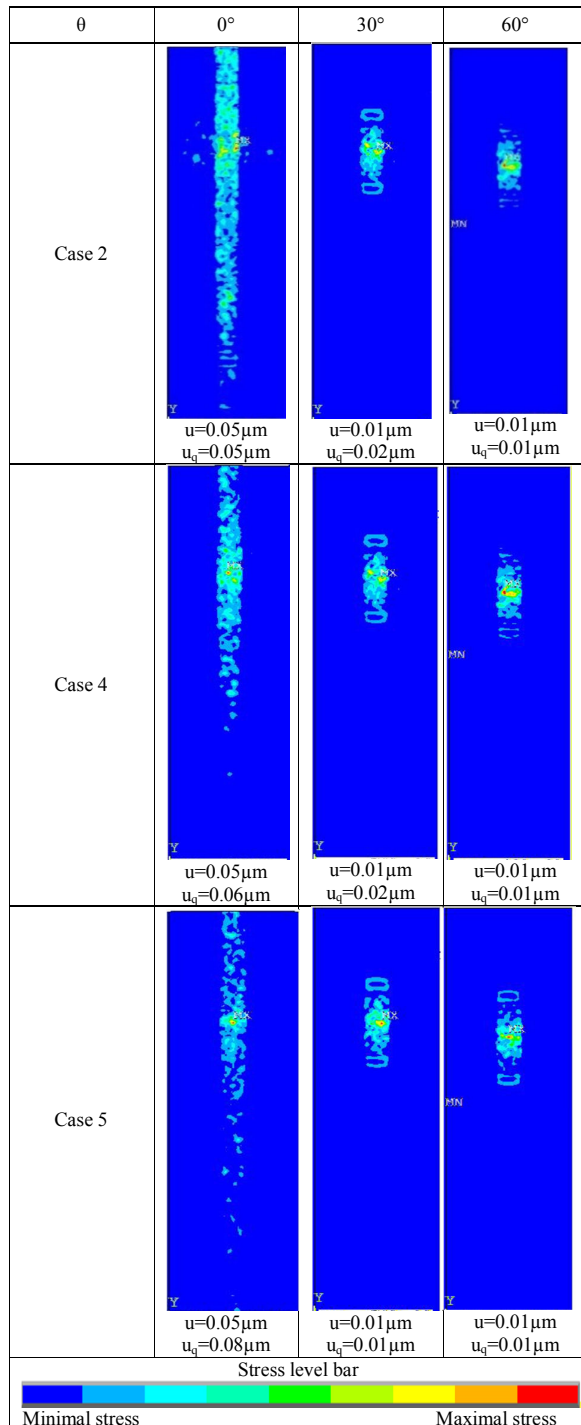
θ	0°	30°	60°
Case 2	u=0.05μm u_q=0.05μm	u=0.01μm u_q=0.02μm	u=0.01μm u_q=0.01μm
Case 4	u=0.05μm u_q=0.06μm	u=0.01μm u_q=0.02μm	u=0.01μm u_q=0.01μm
Case 5	u=0.05μm u_q=0.08μm	u=0.01μm u_q=0.01μm	u=0.01μm u_q=0.01μm
Stress level bar			
Minimal stress			Maximal stress

Fig. 6 Distribution of Von Mises stress under applied displacement *u*.

B. Damage

Fig. 7 illustrates the damages for the case of fiber inclination angle θ=0°. Analyzing the figures, we observe that with the increasing distance of the fiber center to the crack surface from z=0 to z=$50L_c$, there is a little difference in quantity of the broken elements and in the damage distribution pattern (see Figs. 7 (a) and (b)).
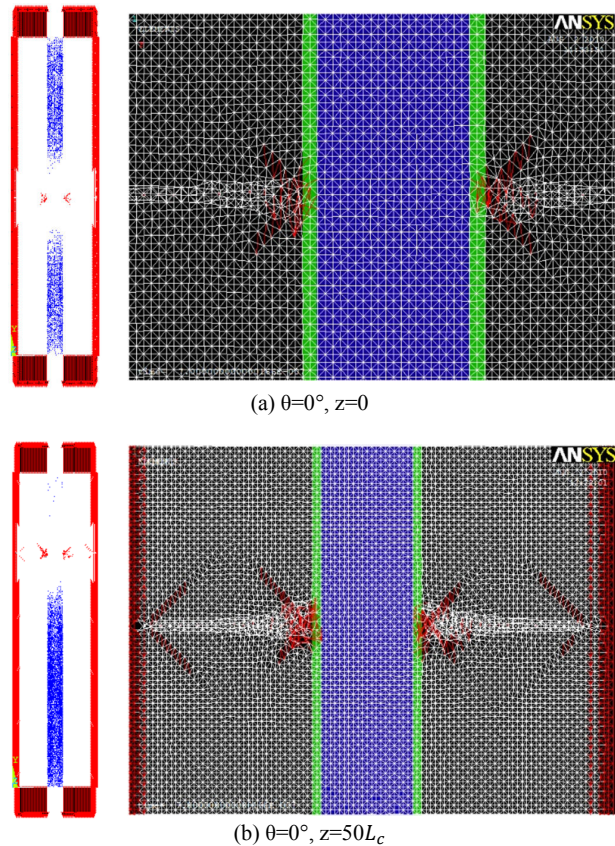

(a) θ=0°, z=0

(b) θ=0°, z=$50L_c$

Fig. 7 Damage in the material: The blue represents elastic elements; the white for the elements that suffer from damage but still load bearing; the red ones are broken totally and lost their capacity of load bearing. The right figures are the amplifications of the center regions of the left figures where the fiber intersects with the crack

Fig. 8 shows the comparison among different inclined angles ((a) θ=0°; (b) θ=60°) and different positions of the fiber center to the crack surface ((b) z=0; (c) z=$50L_c$).

We see clearly that the larger inclined angle, the more damage (Fig. 8 (b) comparing with 8 (a)). Once more we see that the crack position affects damage a little if the crack position is not so near to the fiber end.

Fig. 9 shows the damage at θ=60°, z=$50L_c$, and ds=0.2 μm. We note that although the case 5 represents greater damage in the matrix than the cases 2 and 4, the fiber elements have not been broken. Fig. 9 (e), the amplification of the zone of concentrated damage (Fig. 9 (c)), has confirmed this.

In comparison with the case 4, the damage of the case 2 is less, due to stronger interface in the case 2 than the case 4. However, we have no better explanation for why the case 5 has greater damage than the case 2, even if the case 5 has stronger fiber than the case 2 and stronger interface than the case 4. Maybe stronger fiber leads to less damage in the fiber, then, resulting in higher compression and in consequence, larger damage in the matrix. This needs to be verified in more detailed analysis accounting the fiber damage quantitatively.
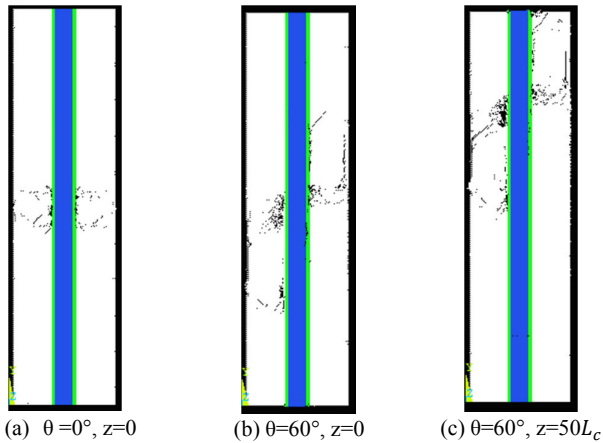
(a) θ =0°, z=0   (b) θ=60°, z=0   (c) θ=60°, z=50L_c

Fig. 8 Damage (black) for the case 2 (steel fiber)

(a) Case 2   (b) Case 4   (c) Case 5   (d) Case 6
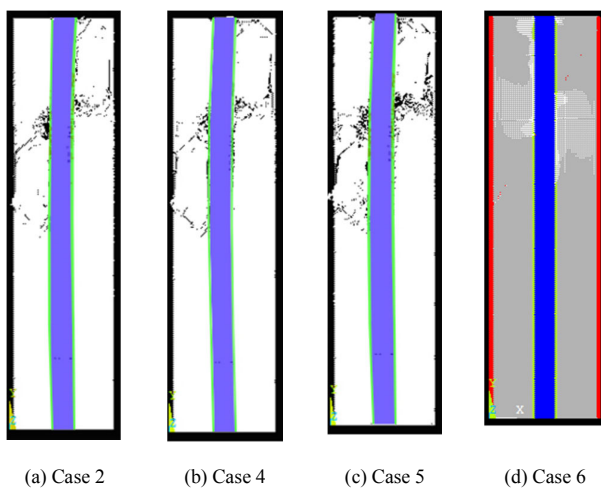

(e) θ=60°, z=50L_c

Fig. 9 Damage comparison: Steel fiber for the cases 2, 4 and 5 and synthetic fiber for the case 6

By comparison with steel fiber (Fig. 9 (c)), although the synthetic fiber has the same strength (1200MPa), its much lower elasticity module makes itself more flexible, permitting a larger critical deformation. Therefore, the synthetic fiber

produces a much lower pressure on the matrix, resulting in quite less damage in the matrix than the steel fiber does.

C. Stress Distribution in Synthetic Fibers

Fig. 10 shows stress distributions for the synthetic fiber. The results for the case 6 is almost same as the case 3, since the difference in the fiber strengths between the case 3 and 6 brings no effect yet in the fiber stress when the stress is too low.
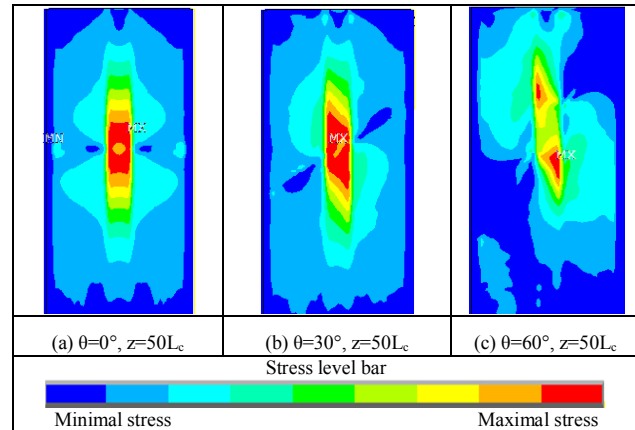

(a) θ=0°, z=50L_c (b) θ=30°, z=50L_c (c) θ=60°, z=50L_c

Stress level bar

Minimal stress   Maximal stress

Fig. 10 Distribution of Von Mises stress for the case 3 where synthetic fiber is employed

D. Bridging Stress

Fig. 11 plots the curves of bridging stress varying with the crack open. It is interested to observe, for the steel fiber cases (cases 2, 4 and 5), the manner of bridging stress increment: up and down alternatively. The stress drops maybe be induced when the damage is substantial in the fiber, demonstrating unload followed by re-loading.

For the case of synthetic fiber (cases 3 and 6), the bridging stress is quite low at almost constant and no up and down happen, because no damage occurs in the fiber due to excellent flexibility of the synthetic fiber.
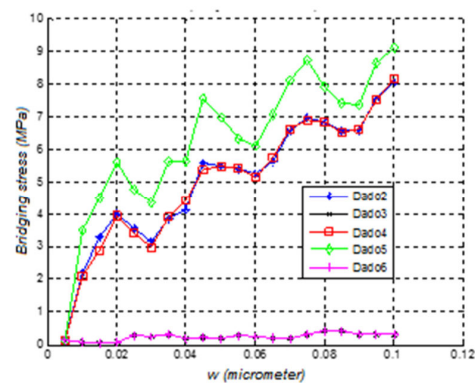

Fig. 11 Bridging stress

VI. Conclusion

This work realized simulation and analysis of toughening in brittle matrix reinforced by fibers, using the discrete element method. By implementation of numerical program, we investigated stress distribution, damage and bridging stress when a crack appeared in the brittle matrix. From the results obtained we conclude:

i. Fibers with high strength and low elasticity module benefit the toughening;

ii. Fibers with high elasticity module relative to the one of the matrix may lead to much damage in the matrix due to spalling effect;

iii. Employment of synthetic fibers of high strength is a good option;

iv. Stiff fibers inclined at large angle relative to the normal vector of the fractured surface could produce large damage;

v. With crack open, bridging stress increases in a manner of up and down. When damage becomes substantial, the stress drops down. This phenomenon cannot be revealed by analytic method.

Fiber toughening in ceramics is complex, involving all of mechanical properties of fiber, matrix and the fiber/matrix interface and fiber geometry. Suitable numerical methods to realize simulation analysis are essential. DEM used in this work has shown its efficiency in the analysis of damage evolution. With the improvement in the computational program, DEM incorporated with FEM may be of more advantage in numerical modeling and simulation for damage evaluation and toughening analysis.

Acknowledgment

References

[1] C. Wang, L. F. Friedrich, "Computational model of effective fibers on toughening in fiber reinforced composites at an early stage of crack formation," in *Proc. 20th Annual International Conference on Composites or Nano Engineering*, Beijing, 2012.

[2] Y. Wang, V. C. Li, S. Backer, "Modelling of fibre pull-out from a cement matrix," *Int. J. Cement Composites Lightweight Concrete*, vol. 10, pp. 143-149, 1988.

[3] V. C. Li, Y. Wang, S. Backer, "A micromechanical model of tension softening and bridging toughening of short random fiber reinforced brittle matrix composites," *J. Mech. Phys. Solids*, vol. 39, pp. 607- 625, 1991.

[4] V. C. Li, "A simplified micromechanical model of compressive strength of fiber-reinforced cementitious composites," *Cement & Concrete Composites*, vol. 14, pp. 131-141, 1992.

[5] Z. Lin, V. C. Li, "Crack bridging in fiber reinforced cementitious composites with slip-hardening interfaces," *J. Mech. Phys. Solids*, vol. 45, pp. 763-787, 1997.

[6] X. Chen, I. J. Beyerlein, L. C. Brinson, "Bridged crack models for the toughness of composites reinforced with curved nanotubes," *J. Mech. Phys. Solids*, vol.59, pp. 1938-1952, 2011.

[7] J. A. Mohandesi, A. Sangghaleh, A. Nazari, N. Pourjavad, "Analytical modeling of strength in randomly oriented PP and PPTA short fiber reinforced gypsum composites," *Computational Materials Science*, vol. 50, pp. 1619-1624, 2011.

[8] J. D. Riera, "Local effects in impact problems on concrete structures," in *Proc. Conference on Structural Analysis and Design of Nuclear Power Plants*, Porto Alegre, Brazil, 1984, Vol. 3, CDU 264.04:621.311.2:621.039.

[9] J. D. Riera, I. Iturrioz, "Discrete element dynamic response of elastoplastic shells subjected to impulsive loading," *Communications in Num. Meth. in Eng.*, vol. 11, pp. 417-426, 1995.

[10] J. D. Riera, I. Iturrioz, "Discrete element model for evaluating impact and impulsive response of reinforced concrete plates and shells subjected to impulsive loading," *Nuclear Engineering and Design*, vol. 179, pp. 135-144, 1998.

[11] L. E. Kosteski, J. D. Riera, I. Iturrioz, R. K. Singh, T. Kant, "Analysis of reinforced concrete plates subjected to impact employing the truss-like discrete element method," *Fatigue & Fracture of Engineering Materials & Structures*, doi: 10.1111/ffe.12227, to be published.

[12] F. Schnaid, L. Spinelli, I. Iturrioz, M. Rocha, "Fracture mechanics in ground improvement design," *Ground Improvement*, vol. 8, pp. 7-15, 2004.

[13] L. F. F. Miguel, I. Iturrioz, J. D. Riera, "Size effects and mesh independence in dynamic fracture analysis of brittle materials," *Computer Methods Modeling in Engineering & Sciences*, vol. 56, pp. 1-16, 2010.

[14] L. A. Dalguer, K. Irikura, J. D. Riera, H. C. Chiu, HC, "The importance of the dynamic source effects on strong ground motion during the 1999 Chi-Chi, Taiwan, earthquake: brief interpretation of the damage distribution on buildings," *Bulletin of the Seismological Society of America*, vol. 91, pp. 1112-1127, 2001.

[15] A. Dalguer, K. Irikura, J. D. Riera, "Generations of New Cracks Accompanied by Dynamic Shear Rupture Propagation of the 2000 Tottori (Japan), Earthquake," *Bulletin of the Seismological Society of America*, vol. 93, pp. 2236-2252, 2003.

[16] R. D. Rios, J. D. Riera, "Size effects in the analysis of reinforced concrete structures," *Engineering Structures*, vol. 26, pp.1115-1125, 2004.

[17] L. F. F. Miguel, J. D. Riera, I. Iturrioz, "Influence of size on the constitutive equations of concrete or rock dowels," *International Journal for Numerical and Analytical Methods in Geomechanics*, vol. 32, pp. 1857-1881, 2008.

[18] I. Iturrioz, L. F. F. Miguel, J. D. Riera JD, "Dynamic fracture analysis of concrete or rock plates by means of the Discrete Element Method," *Latin American Journal of Solids and Structures*, vol. 6, pp. 229-245, 2009.

[19] L. E. Kosteski, I. Iturrioz, R. G. Batista, A. P. Cisilino, "The truss-like discrete element method in fracture and damage mechanics," *Engineering Computations*, vol. 28, pp. 765-787, 2011.

[20] L. E. Kosteski, R. L. Barrios D'Ambra, I. Iturrioz, "Crack propagation in elastic solids using the truss-like discrete element method," *International Journal of Fracture*, vol. 174, pp. 139-161, 2012.

[21] R. L. Barrios D`Ambra, I. Iturrioz, H. Coceres, L. E. Kosteski, T. W. Tech, A. Cisilino, "Cálculo del factor de intensidad de tensiones utilizando el método de los elementos discretos," *Revista Sul-Americana de Engenharia Estrutural*, vol. 4, pp. 7-20, 2007.

[22] L. E. Kosteski, R. Barrios, I. Iturrioz, "Determinación de Parámetros Fractomecánicos Estáticos y Dinámicos utilizando el Método de los Elementos Discretos compuestos por barras," *Revista Internacional Métodos numéricos para cálculo y diseño en ingeniería*, vol. 24, pp. 323-343, 2008.

[23] L. E. Kosteski, R. Barrios, I. Iturrioz, "Fractomechanics parameter calculus using the Discrete Element Method with bars," *Latin American Journal of Solids and Structures*, vol. 6, pp. 301-321, 2009.

[24] M. A. Caravaca, L. E. Kosteski, J. C. Miño, R. L. Barrios D'ambra, B. Uberti, R. A. Casali, "Model for Vickers microhardness prediction applied to SnO2 and TiO2 in the normal and high pressure phases," *Journal of the European Ceramic Society*, vol. 34, pp. 3791–3800, 2014.